Knockout of *c-mos* gene does not affect tumor progression in murine models of lung and colorectal cancer

Zhengxi Chen [1], **Ju Qiao** [2], **Zhenqi Chen** Corresp., [1], **Qian Xiao** Corresp. [3]

[1] Department of Orthodontics, Shanghai Ninth People's Hospital, Shanghai Jiao Tong University, Shanghai, China

[2] Department of Mechanical and Industrial Engineering, Northeastern University, Boston, USA

[3] Department of Pharmacology, Yale University, New Haven, Connecticut, USA

Corresponding Authors: Zhenqi Chen, Qian Xiao
Email address: orthochen@yeah.net, qian.xiao@yale.edu

Background. The *c-mos* proto-oncogene was one of the first proto-oncogenes to be cloned. Apart from its role in meiosis, many efforts have been made to illuminate the mechanisms by which *c-mos* acts as an oncogene. *c-mos* or its coding messenger RNA have been confirmed in most somatic tissues at low levels. However, a detailed role of *c-mos* as an oncogene in somatic cells remains unknown.

Methods. In this study, we analyzed online databases to find out the correlation between Mos expression and poor survival rates in human cancer patients. Then, we investigated whether the involvement of *c-mos* in tumor progression via applying Apc^{min} intestinal cancer model and $Kras^{G12D}$ lung cancer model.

Results. First, we found the expression of Mos differed between human and mice, and a significant correlation between high Mos expression and poor survival rates in lung cancer patients. Interestingly, we tested that the effects of deficient *c-mos* in both Apc^{min} intestinal cancer model and $Kras^{G12D}$ lung cancer model. Despite the abovementioned significant correlation, the results did not show a strong inhibitory effect on murine models of lung and intestine tumors. We find no evidence of a direct role for *c-mos* in tumor progression in abovementioned mice models.

Discussion. It indicated that functions of c-mos gene might be species-specific and that *c-mos* involvement in tumor progression was circumstantial and it probably depended on other oncogene activation.

Keywords: *c-mos*, Kras, Apc, survival rate, murine model, lung cancer, colorectal cancer

Knockout of *c-mos* gene does not affect tumor progression in murine models of lung and colorectal cancer

Zhengxi Chen[1,3], Ju Qiao[2], Zhenqi Chen[3*], Qian Xiao[1*]

1 Department of Pharmacology, School of Medicine, Yale University, New Haven, CT, USA

2 Department of Mechanical and Industrial Engineering, Northeastern University, Boston, MA, USA

3 Department of Orthodontics, Ninth People's Hospital, School of Stomatology, Shanghai key Laboratory of Stomatology, Shanghai Jiao Tong University, Shanghai, China

Corresponding Author: Dr. Zhenqi Chen and Dr. Qian Xiao

Zhenqi Chen*

500 Quxi Rd, Huangpu District, Shanghai, 200011, China

Email address: orthochen@yeah.net

Qian Xiao*

10 Amistad St, New Haven, CT, 06519, USA

Email address: qian.xiao@yale.edu

Abstract

Background. The *c-mos* proto-oncogene was one of the first proto-oncogenes to be cloned. Apart from its role in meiosis, many efforts have been made to illuminate the mechanisms by which *c-mos* acts as an oncogene. *c-mos* or its coding messenger RNA have been confirmed in most somatic tissues at low levels. However, a detailed role of *c-mos* as an oncogene in somatic cells remains unknown.

Methods. In this study, we analyzed online databases to find out the correlation between Mos expression and poor survival rates in human cancer patients. Then, we investigated whether the involvement of *c-mos* in tumor progression via applying Apc^{min} intestinal cancer model and $Kras^{G12D}$ lung cancer model.

Results. First, we found the expression of Mos differed between human and mice, and a significant correlation between high Mos expression and poor survival rates in lung cancer patients. Interestingly, we tested that the effects of deficient *c-mos* in both Apc^{min} intestinal cancer model and $Kras^{G12D}$ lung cancer model. Despite the abovementioned significant correlation, the results did not show a strong inhibitory effect on murine models of lung and intestine tumors. We find no evidence of a direct role for *c-mos* in tumor progression in abovementioned mice models.

Discussion. It indicated that functions of c-mos gene might be species-specific and that *c-mos* involvement in tumor progression was circumstantial and it probably depended on other oncogene activation.

Keywords: *c-mos*, Kras, Apc, survival rate, murine model, lung cancer, colorectal cancer

Introduction

At the molecular level, emerging oncogene paradigm has been proved to be a powerful tool in answering the questions concerning the nature of tumorigenesis in human and laboratory animals. Proto-oncogenes, known as oncogenes in the non-activated state, probably regulate cell growth and differentiation. A direct evidence for the involvement of proto-oncogenes in cancer was that the behavior of retroviruses carrying activated oncogenes directly implicated in tumorigenesis in animal models.

One of the first proto-oncogenes to be cloned was the *c-mos* gene of which the product was Mos, a member of the serine/threonine kinase family (Oskarsson et al., 1980). According to the previous study (Dupré et al., 2002), as the synthesis of Mos was specifically regulated and restricted in time and cell types, the expression of Mos was hardly detected in somatic cells except in germ cells. Thus, much of the research concerning Mos has been focused on its role in meiosis. Mos is strictly necessary for the first meiotic division of oocytes and then regulates a critical checkpoint function during metaphase II (Sagata et al., 1989). There are several comprehensive reviews available on this topic (Singh & Arlinghaus, 1997; Sagata, 1997; Yew, Strobel & Vande, 1993).

During the past 30 years, many efforts have been made to illuminate the mechanisms by which *c-mos* acts as an oncogene. *c-mos* or its coding messenger RNA have been confirmed in most somatic tissues at low levels (Herzog et al., 1989; Propst et al., 1987; Li et al., 1993). Overexpression of *c-mos* has been found in 27% of human non-small cell lung carcinomas. Tumors from stages II/III have higher Mos expression than tumors form stage I patients

(Gorgoulis et al., 2001). *c-mos* is also the one of identified 18 kinase and kinase-related genes whose overexpression can substitute for EGFR in EGFR dependent lung adenocarcinomas (Sharifnia et al., 2014). Lidereau *et al.* found the breast cancer patients had a higher percentage of polymorphism in the *c-mos* locus which caused the activation of the *c-mos* proto-oncogene in breast tumors (Lidereau et al., 1985) than the leukemia patients. Vitale *et al.* revealed that Mos was upregulated in colon cancer cells after spindle damage (Vitale et al., 2010). Recent studies identified Mos pathway in human colorectal cancers (CRCs) (Centelles, 2012) and confirmed that Mos-mitogen-activated protein kinase pathway was activated in irradiated *p53*-mutant lymphoma cells (Erenpreisa & Wheatley, 2005; Erenpreisa, Kalejs & Cragg, 2005). Moreover, upregulation of Mos was observed in genotoxically stressed lymphoma and human breast cancer cell lines (Erenpreisa, Kalejs & Cragg MS,2005; Kalejs et al., 2006; Ianzini et al., 2009; Erenpreisa et al., 2009). However, a detailed role of *c-mos* as an oncogene in somatic cells remains unknown.

Herein, the study was aimed to investigate whether *c-mos* is involved in tumor progression. We first took advantage of online databases and found the expression of Mos differed between human and mice. There was also a significant correlation between high Mos expression and poor survival rates in lung cancer patients. To better unveil the biological function of Mos in characterized cancers, we examined the effects of deficient *c-mos* in both Apc^{min} intestinal cancer model and $Kras^{G12D}$ lung cancer model as well.

Materials and Methods

Experimental animals

Mos^{tm1Ev} (B6.129S6-Mostm1Ev/J), *Apc*$^{Min/+}$ (C57BL/6J-ApcMin/J) and *Kras*$^{LSL-G12D}$ (B6.129S4-Krastm4Tyj/J) mice were acquired from Jackson Laboratory. *Kras*$^{LSL-G12D}$ and *Mos*^{tm1Ev} mice were backcrossed to *C57BL/6J* for 3 generations. Lung cancer mice models with *Kras*$^{LSL-G12D}$ & *Mos*^{tm1Ev} (*Kras*^{G12D}, *Mos*$^{-/-}$) were generated by crossing *Kras*$^{LSL-G12D}$ with *Mos*^{tm1Ev} mice. Intestine cancer mice model *Apc*$^{Min/+}$ & *Mos*^{tm1Ev} (*Apc*$^{Min/+}$, *Mos*$^{-/-}$) mice were generated by crossing *Apc*$^{Min/+}$ with *Mos*^{tm1Ev} mice. All animals were cared for in strict accordance with National Institutes of Health (USA) guidelines and all procedures were approved by the Yale University Animal Care and Use Committee.

Mouse tumor model

For *de novo* lung cancer mice model, *Kras*^{G12D} (n=11, male), and *Kras*^{G12D}, *Mos*$^{-/-}$ (n=9, male) mice were treated with 2x10^{6} plague-forming unites of Adeno-Cre injected intranasally at 8 weeks of age (weight around 18g) as previously described (Gao et al., 2010; Xiao et al., 2015; DuPage, Dooley & Jacks, 2009) (Fig 1). After 12 weeks, mice were sacrificed in CO2 Rodent Euthanasia Chamber for gross inspection and histopathological. Lung tumors were dissected for histopathological analysis. Intestine cancer mice models with *Apc*$^{Min/+}$(n=5, male), *Apc*$^{Min/+}$, *Mos*$^{-/-}$ (n=5, male) mice were housed for 20 weeks, then mice were sacrificed in CO2 Rodent Euthanasia Chamber and intestine tissues were collected for histopathological examination. Tumor number and tumor size were measured. All mice were monitored twice a week until endpoint time of the experiment. No animals were excluded from the analysis.

Quantitative RT-PCR

Lung and intestine samples were collected and total RNA was isolated with RNeasy Plus Mini Kit (QIAGEN) according to the manufacturer's instructions. Complementary DNAs were synthesized from the above-mentioned collected RNAs using the iScript cDNA Synthesis Kit (Bio-Rad). Quantitative PCR was done using IQ™ SYBR Green super-mixes and CFX96™ Touch Real-Time PCR detection system (Bio-rad). For all quantitative PCR reactions, Gapdh was measured for an internal control and used to normalize the data. The PCR primers used were as follows: c-mos: 5'-CTCCGGAGATCCTGAAAGGA-3' (sense) and 5'-CAGTGTCTTTCCAGTCAGGG-3' (antisense). Gapdh: 5'-TGCCCCCATGTTTGTGATG-3' (forward) and 5'-TGTGGTCATGAGCCCTTCC′ (reverse).

Histopathological analysis

Histopathological analysis was performed according to our previous study [20, 21]. In short, after mice were sacrificed, lungs were inflated with 1 ml Bouin's solution (Sigma-Aldrich) at room temperature for 20 min and fixed in 20 ml 4% PFA at 4°C for 24 h. Fixed lung tissues were embedded in paraffin sectioned at 5 μm thickness for hematoxylin and eosin (HE) staining.

Correlation of Mos expression and patient survival in lung cancers

The Mos expression and overall survival data were obtained from Kaplan-Meier survival plotter datasets as of April 20, 2017. The high and low Mos (221367_at) expressers were grouped using an arbitrary cutoff percentile of 50% (966 for low Mos expressers, and 960 for high Mos expressers). The Mantel-Cox Log-Rank tests were done using the GraphPad Prism 7 software.

Correlation of mos expression and patient survival in colorectal cancers

The Mos expression and overall survival data were obtained from TCGA datasets (Nature 2012). The high and low Mos expressers were grouped using an arbitrary cutoff percentile of 50% (110 for low Mos expressers, and 109 for high Mos expressers). The Mantel-Cox Log-Rank tests were done using GraphPad Prism 7 (GraphPad Software, La Jolla, CA, USA).

Study design and Statistical analysis

Minimal group size for tumor progression studies was calculated using an online power calculator available from DSS Researcher's Toolkit with an α of 0.05 and power of 0.8. Animal groups were not blinded but randomized, and investigators were blinded to the tumor counting experiments. No samples or animals were excluded from the analysis. Hypothesis concerning the data which included normal distribution and similar variation between the experimental groups were examined for appropriateness before the conduct of statistical tests. All statistical analyses were performed with Student's t-test (two groups) or ANOVA (multiple groups) using SPSS version 21.0, software (IBM Corp, Armonk, NY).

Results

Mos expression from publicly available database

According to the publicly available BIOGPS database (http://www.biogps.org) records, *c-mos* was found to be expressed almost evenly in human tissues (Fig 2A), while it expressed significantly higher in ovaries than other tissues in mice (Fig 3D).

Analysis of the TCGA Lung 2 cohort in the Oncomine database (www.oncomine.org) showed that Mos expression was significantly upregulated in human lung adenocarcinoma samples than in the non-tumorous lung tissues (Fig 2B). In addition, analysis of the datasets

obtained from Kaplan-Meier survival plotter revealed there might be a significant correlation between high Mos expression and poor survival rates (Fig 3C). The expression of Mos in human CRCs implicated that both human colon and rectal adenocarcinoma tissues had higher Mos expression (Fig 2D), although the correlation of high Mos expression with poor survival rates was a very slight trend toward significance (Fig 2E).

Genetic deletion of *c-mos* gene has no effect on intestine and lung morphogenesis

Before the establishment of the lung cancer and intestine tumor animal model, the *c-mos* deficiency was confirmed in both lung and small intestine tissues using Real-time PCR quantification (Fig 3A). Morphological changes of lung and small intestine in both $Mos^{-/-}$ and *WT* mice were observed at the age of 12 months. No significant differences were shown with regard to the tissue size, weight, and macroscopic appearance. The histological structures of lung and small intestine in $Mos^{-/-}$ and *WT* mice were nearly identical (Fig 3B and 3C).

Genetic deletion of *c-mos* gene has no significant effect on tumor burden in $Kras^{G12D}$ mice

There was a trend on the slowdown of tumor progression in *c-mos* deficient mice, but it was not significant (Fig 4A-B). Fig 3C showed representative histological sections from the $Kras^{G12D}$ mice and the $Kras^{G12D}$; $Mos^{-/-}$ mice. Further analysis showed Mos expression had concurrence with Kras, EGFR, TP53 and BRAF, but only correlated with RET significantly (p= 0.0113) (data not shown).

Genetic deletion of *c-mos* gene has no inhibitory effect on colorectal tumor progression in $APC^{Min/+}$ mice

Then, the role of mos-deficiency in tumor formation was investigated using the *Apc*$^{Min/+}$ mouse intestinal tumor model. We found that there was no inhibitory effect on colon tumor progression when the *c-mos* gene was absent (Fig 4F-G), and the absence of *c-mos* gene had no influence on small intestinal tumor burdens in *Apc*$^{Min/+}$ mice neither (Fig 4D-E).

Discussion

Although the *c-mos* gene has been known to be involved in the control of meiosis and mitosis for more than three decades (Herzog et al., 1989; Propst et al., 1987; Li et al., 1993), our understanding of its protein product Mos and its role in somatic cells on the mechanisms by which Mos could act as an oncogene is still incomplete. Web-based databases and data-mining platforms such as BIOGPS and Oncomine have been proved as a powerful tool for the cancer research community (Rhodes et al., 2004). In this study, we initially took advantage of these databases and found the expression of Mos in human differs from mice. In human, the expression of Mos was relatively even in different organs whilst Mos expression was higher in ovary than in other organs in mice. These results indicated that *c-mos* might have some species-specific effects. The analysis also suggested that Mos expression was significantly upregulated in human lung adenocarcinoma samples than in the non-tumorous lung tissue with a significant correlation between high Mos expression and poor survival rates. Human colon and rectal adenocarcinoma tissues also had higher Mos expression with an apparent significant correlation between high Mos expression and poor survival rates. These results seemed to support that Mos might promote tumor progression.

Given this, we first tested biological function of the *c-mos* gene in tumor progression in the $Apc^{Min/+}$ mouse which was regarded as a good model to study multistage colon carcinogenesis (Yamada & Mori, 2007). Besides, we also investigated the role of *c-mos* deficiency in the formation of lung tumors using the $Kras^{G12D}$ mice which was suggested as a classic model for the experimental study of lung cancer (Gao et al., 2010; Xiao et al., 2015). No significant changes of the tissue size, weight, and macroscopic appearance were found in lung tissue in $c\text{-}mos^{-/-}$ mice via gross morphological observations. Regarding multiple driver oncogenes in human NSCLCs that included but not were limited to KRAS, EGFR, ALK, RET, BRAF, PIK3CA, MET, HER2, ROS1, MEK1, NRAS and AKT1, the concurrence patterns of *c-mos* expression with Kras, EGFR, TP53 and BRAF were found in this study, however, only the correlation with RET showed significant pattern. It suggested that the functions of *c-mos* in Kras, EGFR, TP53 or BRAF which drove NSCLCs could be substituted by other pathways in a compensating way. Also, according to previous studies (Kohno et al., 2012; Lewis et al., 1998), approximately 1.3% of lung tumors evaluated had chromosomal changes which led to the occurrence of RET gene fusion. These gene rearrangements occurred almost in the entire adenocarcinoma tumors. RET fusions had been found in tumors without other frequent driver oncogenes (e.g., EGFR, KRAS, and ALK) as well. Although RET fusions are confirmed to be oncogenic both *in vitro* and *in vivo*, the functional consequences of RET fusion related proteins in lung adenocarcinoma are still not fully understood. In addition, in human NSCLC, there is a connection between *c-mos* expression and *p53* status, genomic instability and tumor kinetics. This indicated that *c-mos* might play an important role in RET-driven lung cancers via its gene rearrangements.

Our results demonstrated that in *Apc*$^{Min/+}$ mice, colorectal tumor burdens were slightly reduced by *c-mos* deficiency. It might share some characteristics with the human's colorectal adenocarcinoma. In human, *c-mos* was significantly upregulated in colorectal adenocarcinoma tissues and presented slight concurrence with APC and TP53 while mutually exclusive with Kras. The *c-mos*/MKK/ERK pathway has been linked to the cellular processes like growth and differentiation (Mansour et al., 1994; Benayoun et al., 1998; Sagata et al., 1998). Given the diversity of pathways in colon cancers, and the fact that ERKs could be activated by numerous upstream signals (Mansour et al., 1994), our observation might imply *c-mos*/ERK pathway could just be one of the alternative activation modes of the Ras/Raf/MEK/ERK pathway which participated in colorectal cancer progression. Our results also showed a variation in inhibitive effects of Mos between murine and human tumors which might be attributed to the species-specific differences. There was some substantiated evidence interpreted that Mos played different roles in different species. In *Xenopus* oocyte maturation, as an active component of a cytostatic factor, Mos was required for the activation of maturation promoting factor, germinal vesicle breakdown and the extrusion of the first polar body as well (Sagata et al., 1998). In contrast, the phenotype of *c-mos* mutant mice suggested that Mos was needed to arrest developing oocytes in metaphase II only in murine species (Colledge et al., 1994; Hashimoto et al., 1994). These data all indicated that functions of the *c-mos* gene might be species-specific. In that the mysteries of the human body still remained unraveled, we suspected that the functions of *c-mos* in us, humans, might be a vulnerable target for cancer induction but not in mice.

Conclusion

In summary, our study deals with the biological functions of *c-mos* and its relationship to tumor progression of which the results have yielded several findings. First, analysis from online database showed Mos expression was significantly upregulated in human lung adenocarcinoma and colorectal adenocarcinoma samples than those from non-tumorous tissues. On the one hand, there was a significant correlation between high Mos expression with poor survival rates in patients with lung cancer. These results indicated that Mos might play an important role in lung adenocarcinoma and colorectal tumor progression. Therefore, we established the mice model characterized by $Kras^{G12D}$ lung and Apc^{min} intestine tumor. Although *c-mos* deficiency didn't show a strong inhibitory effect on lung and intestine tumor progression, our study still did shed some light on future research based on the findings that *c-mos* involvement in tumor progression was circumstantial and it probably depended on other oncogene activation.

Conflict of interest

No conflicts of interest, financial or otherwise, are declared by the authors.

Acknowledgement

Thanks to Michelle Orsulak for technical assistance.

References

Benayoun B, Pelpel K, Solhonne B, Guillier M, Leibovitch SA. 1998. Overexpression of Mos(rat) proto-oncogene product enhances the positive autoregulatory loop of MyoD. *FEBS Lett.* 437:39-43.

Centelles JJ. 2012. General aspects of colorectal cancer. *ISRN Oncol.* 2012:139268.

Colledge WH, Carlton MB, Udy GB, Evans MJ. 1994. Disruption of c-mos causes parthenogenetic development of unfertilized mouse eggs. *Nature.*370:65-68.

242 DuPage M, Dooley AL, Jacks T. 2009. Conditional mouse lung cancer models using adenoviral
243 or lentiviral delivery of Cre recombinase. *Nat Protoc*. 4:1064-1072.

244 Dupré A, Jessus C, Ozon R, Haccard O. 2002. Mos is not required for the initiation of meiotic
245 maturation in Xenopus oocytes. *EMBO J*. 21:4026-4036.

246 Erenpreisa J, Wheatley D. 2005. Endopolyploidy in development and cancer; survival of the
247 fattest'? *Cell Biol Int.* 29:981-982.

248 Erenpreisa J, Kalejs M, Cragg MS. 2005. Mitotic catastrophe and endomitosis in tumor cells: an
249 evolutionary key to a molecular solution. *Cell Biol Int.* 29:1012-1018.

250 Erenpreisa J, Cragg MS, Salmina K, Hausmann M, Scherthan H. 2009. The role of meiotic
251 cohesin REC8 in chromosome segregation in gamma irradiation-induced endopolyploid tumor
252 cells. *Exp Cell Res*. 315:2593-2603.

253 Gao Y, Xiao Q, Ma H, Li L, Liu J, et al. 2010. LKB1 inhibits lung cancer progression through
254 lysyl oxidase and extracellular matrix remodeling. *Proc Natl Acad Sci USA*. 107:18892-18897.

255 Gorgoulis VG, Zacharatos P, Mariatos G, Liloglou T, Kokotas S, et al. 2001. Deregulated
256 expression of c-mos in non-small cell lung carcinomas: relationship with p53 status, genomic
257 instability, and tumor kinetics. *Cancer Res*. 61:538-549.

258 Hashimoto N, Watanabe N, Furuta Y, Tamemoto H, Sagata N, et al. 1994. Parthenogenetic
259 activation of oocytes in c-mos-deficient mice. *Nature*. 370:68-71.

260 Herzog NK, Ramagli LS, Khorana S, Arlinghaus RB. 1989. Evidence for somatic cell expression
261 of the c-mos protein [corrected]. *Oncogene*. 4:1307-1315.

262 Ianzini F, Kosmacek EA, Nelson ES, Napoli E, Erenpreisa J, et al. 2009. Activation of meiosis-
263 specific genes is associated with depolyploidization of human tumor cells following radiation-
264 induced mitotic catastrophe. *Cancer Res*. 69:2296-2304.

265 Kalejs M, Ivanov A, Plakhins G, Cragg MS, Emzinsh D, et al. 2006. Upregulation of meiosis-
266 specific genes in lymphoma cell lines following genotoxic insult and induction of mitotic
267 catastrophe. *BMC Cancer*. 6:6.

268 Kohno T, Ichikawa H, Totoki Y, Yasuda K, Hiramoto M, et al. 2012. KIF5B-RET fusions in lung
269 adenocarcinoma. *Nat Med*. 18:375-377.

270 Lewis TS, Shapiro PS, Ahn NG. 1998. Signal transduction through MAP kinase cascades. *Adv*
271 *Cancer Res*.74:49-139.

272 Li CC, Chen E, O'Connell CD, Longo DL. 1993. Detection of c-mos proto-oncogene expression
273 in human cells. *Oncogene*. 81:685-1691.

Lidereau R, Mathieu-Mahul D, Theillet C, Renaud M, Mauchauffé M, et al. 1985. Presence of an allelic EcoRI restriction fragment of the c-mos locus in leukocyte and tumor cell DNAs of breast cancer patients. *Proc Natl Acad Sci U S A*. 82:7068-7070.

Mansour SJ, Matten WT, Hermann AS, Candia JM, Rong S, et al. 1994. Transformation of mammalian cells by constitutively active MAP kinase kinase. *Science*. 265:966-970.

Oskarsson M, McClements WL, Blair DG, Maizel JV, Vande Woude GF. 1980. Properties of a normal mouse cell DNA sequence (sarc) homologous to the src sequence of Moloney sarcoma virus. *Science*. 207:1222-1224.

Propst F, Rosenberg MP, Iyer A, Kaul K, Vande Woude GF. 1987. c-mos proto-oncogene RNA transcripts in mouse tissues: structural features, developmental regulation, and localization in specific cell types. *Mol Cell Biol*. 7:1629-1637.

Q Xiao, Y Jiang, Q Liu, J Yue, C Liu, et al. 2015.Minor Type IV Collagen α5 Chain promotes cancer progression through discoidin domain receptor-1. *PLoS genetics* 11: e1005249.

Rhodes DR, Yu J, Shanker K, Deshpande N, Varambally R, Ghosh D, et al. 2004. ONCOMINE: a cancer microarray database and integrated data-mining platform. *Neoplasia*. 6:1-6.

Sagata N, Daar I, Oskarsson M, Showalter SD, Vande Woude GF. 1989a. The product of the mos proto-oncogene as a candidate 'initiator' for oocyte maturation. *Science.* 245:643-646.

Sagata N, Oskarsson M, Copeland T, Brumbaugh J, Vande et al. 1998. Function of c-mos proto-oncogene product in meiotic maturation in Xenopus ocytes. *Nature*. 335: 519-525.

Sagata N. 1997. What does mos do in oocytes and somatic cells? *Bioessays*.19:13-21.

Sharifnia T, Rusu V, Piccioni F, Bagul M, Imielinski M, et al. 2014. Genetic modifiers of EGFR dependence in non-small cell lung cancer. *Proc Natl Acad Sci U S A*. 111:18661-18666.

Singh B, Arlinghaus RB. 1997. Mos and the cell cycle. *Prog Cell Cycle Res*. 3:251-259.

Vitale I, Senovilla L, Jemaà M, Michaud M, Galluzzi L, et al. 2010. Kroemer G. Multipolar mitosis of tetraploid cells: inhibition by p53 and dependency on Mos. *EMBO J.* 7:1272–1284.

Yamada Y, Mori H. 2007. Multistep carcinogenesis of the colon in Apc(Min/+) mouse. *Cancer Sci*. 98:6-10.

Yew N, Strobel M, Vande Woude GF.1993. Mos and the cell cycle:the molecular basis of the transformed phenotype. *Curr Opin Genet Dev*. 3:19-25.

Figure Legend

Fig 1. The schematic diagram of intranasal delivery.

Fig 2. *c-mos* expression in human normal and cancer tissues.
(A) Analysis of GeneAtlas U133A, gcrma in the BioGPS database (http://biogps.org) revealed that c-mos expression is present in human tissues. (B) Analysis of the TCGA Lung 2 cohort in the Oncomine database (www.oncomine.org) revealed that c-mos expression was significantly upregulated in human lung adenocarcinoma samples than the non-tumorous lung tissues. (C) Correlation between c-mos expression and patient survival. The c-mos expression and overall survival data were obtained from Kaplan-Meier survival plotter datasets as of April 20, 2017. The high and low c-mos (221367_at) expressers were grouped using an arbitrary cutoff percentile of 50% (966 for low c-mos expressers, and 960 for high c-mos expressers). The Mantel-Cox Log-Rank tests were done using the GraphPad Prism 7 software. (D) Analysis of the TCGA Colorectal 2 cohort in the Oncomine database (www.oncomine.org) revealed that c-mos expression was significantly upregulated in human colon and rectal adenocarcinoma samples than the non-tumorous colon tissues. (E) Correlation between c-mos expression and patient survival. The c-mos expression and overall survival data were obtained from TCGA datasets (Nature 2012). The high and low c-mos expressers were grouped using an arbitrary cutoff percentile of 50% (110 for low c-mos expressers, and 109 for high c-mos expressers). The Mantel-Cox Log-Rank tests were done using the GraphPad Prism 7 software.

Fig 3. Genetic deletion of c-mos gene has no effect on intestine and lung morphogenesis
(A) Real-time PCR quantification of c-mos mRNA levels in mouse lung and intestine tissues with wild-type (n=3) and with c-mos deficiency (n=3). Data were presented as means ± SEM. Statistical analyses were performed using Two-way ANOVA. (B) H&E staining of the lung from wild-type and c-mos-/- mice with regular architecture. (C) Representative H&E staining of

intestine from wild-type and c-mos-/- mice intestine. Scale bars: 50μm. (D) Analysis of GeneAtlas MOE430, gcrma in the BioGPS database (http://biogps.org) revealed that c-mos expression is present in most mouse tissues but significantly higher in ovaries.

Fig 4. Genetic deletion of c-mos gene has on effect on tumor burden in both of KrasG12D lung cancer mice model and APCMin/+ intestine cancer mice model

(A-B) Tumor development in c-mos knockout and wild-type (WT) within KrasG12D mutation. Animals showed spontaneous lung tumor development at 5 months' age. A. Total number of lung surface tumor. (B) Number of large tumor based on tumor size (diameter >2 mm). (C) Histological confirmation of tumor development. Scale bars: 100μm. Data are presented as means ± SEM. N=9-11, Student's t-test. D-E. Tumor development in c-mos knockout and wild-type (WT) within APCmin/+ animals. Animals showed spontaneous intestine tumor development at 5 months' age. (D) Total number of small intestine tumors. E. Number of the intestine tumor based on polys size. (F) Total number of colon tumor. (G) Number of colon tumor based on polys size. Data are presented as means ± SEM. N=5, Two-way ANOVA.

Figure 1

The schematic diagram of intranasal delivery

The schematic diagram of intranasal delivery

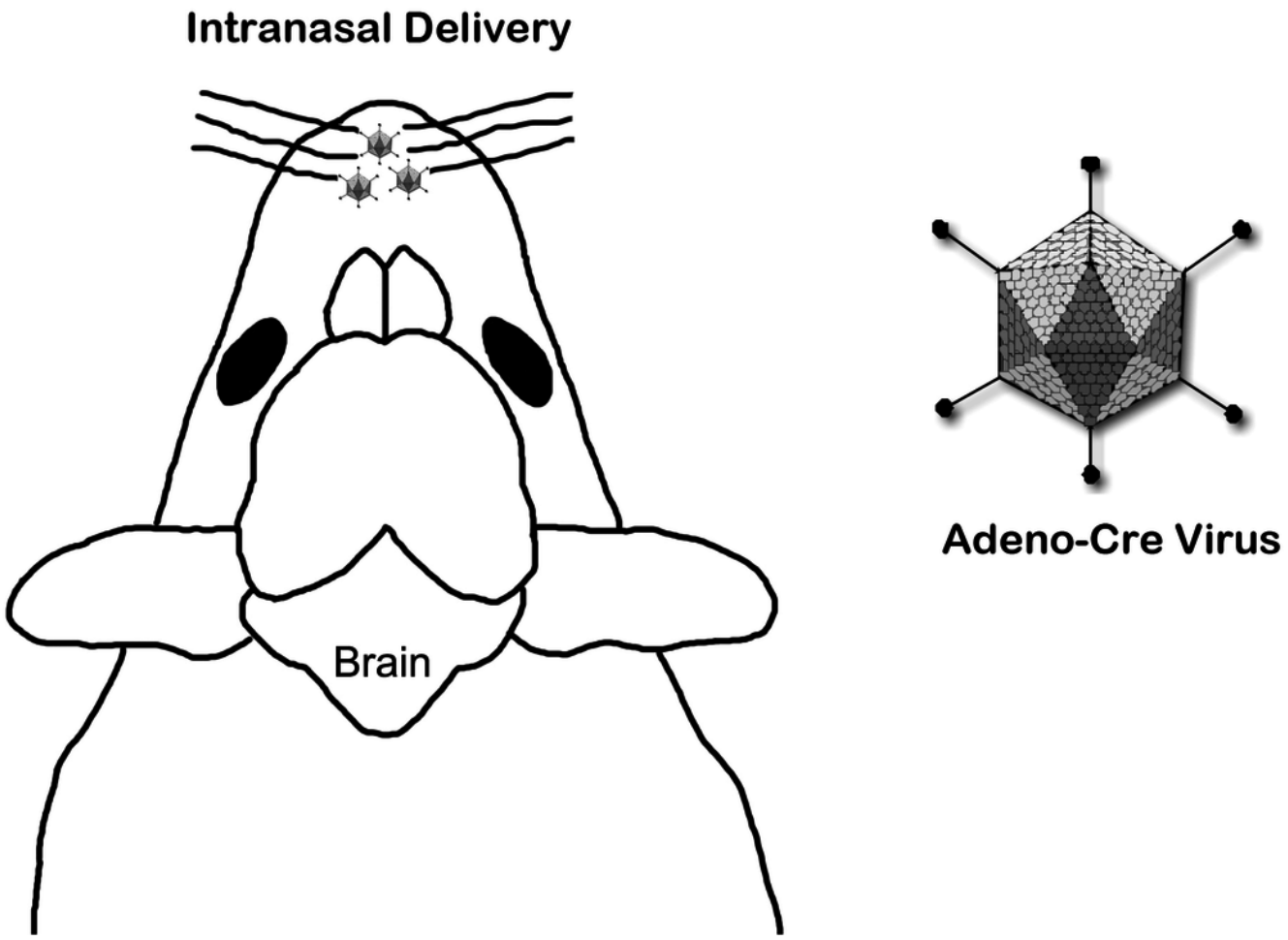

PeerJ Preprints | https://doi.org/10.7287/peerj.preprints.3426v1 | CC BY 4.0 Open Access | rec: 22 Nov 2017, publ: 22 Nov 2017

Figure 2

c-mos expression in human normal and cancer tissues

(A) Analysis of GeneAtlas U133A, gcrma in the BioGPS database (http://biogps.org) revealed that c-mos expression is present in human tissues. (B) Analysis of the TCGA Lung 2 cohort in the Oncomine database (www.oncomine.org) revealed that c-mos expression was significantly upregulated in human lung adenocarcinoma samples than the non-tumorous lung tissues. (C) Correlation of c-mos expression and patient survival. The c-mos expression and overall survival data were obtained from Kaplan-Meier survival plotter datasets as of April 20, 2017. The high and low c-mos (221367_at) expressers were grouped using an arbitrary cutoff percentile of 50% (966 for low c-mos expressers, and 960 for high c-mos expressers). The Mantel-Cox Log-Rank tests were done using the GraphPad Prism 7 software. (D) Analysis of the TCGA Colorectal 2 cohort in the Oncomine database (www.oncomine.org) revealed that c-mos expression was significantly upregulated in human colon and rectal adenocarcinoma samples than the non-tumorous colon tissues. (E) Correlation of c-mos expression and patient survival. The c-mos expression and overall survival data were obtained from TCGA datasets (Nature 2012). The high and low c-mos expressers were grouped using an arbitrary cutoff percentile of 50% (110 for low c-mos expressers, and 109 for high c-mos expressers). The Mantel-Cox Log-Rank tests were done using the GraphPad Prism 7 software.

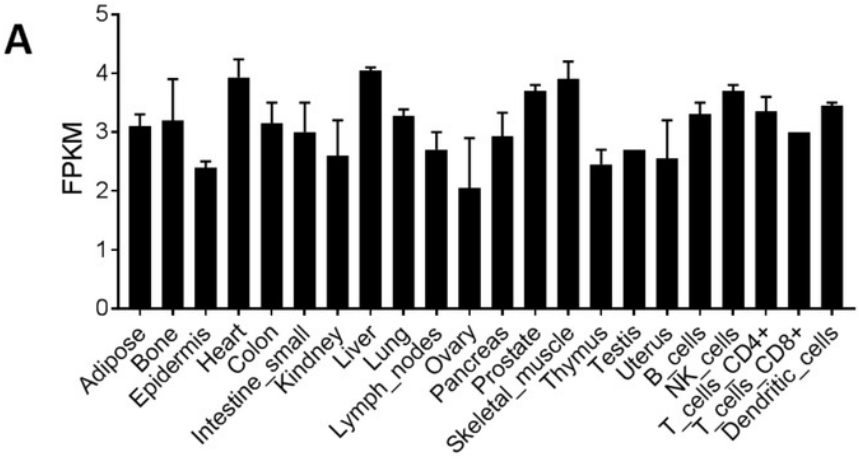
A
FPKM
0
1
2
3
4
5
Adipose
Bone
Epidermis
Heart
Colon
Intestine_small
Kindney
Liver
Lung
Lymph_nodes
Ovary
Pancreas
Prostate
Skeletal_muscle
Thymus
Testis
Uterus
B_cells
NK_cells
T_cells_CD4+
T_cells_CD8+
Dendritic_cells

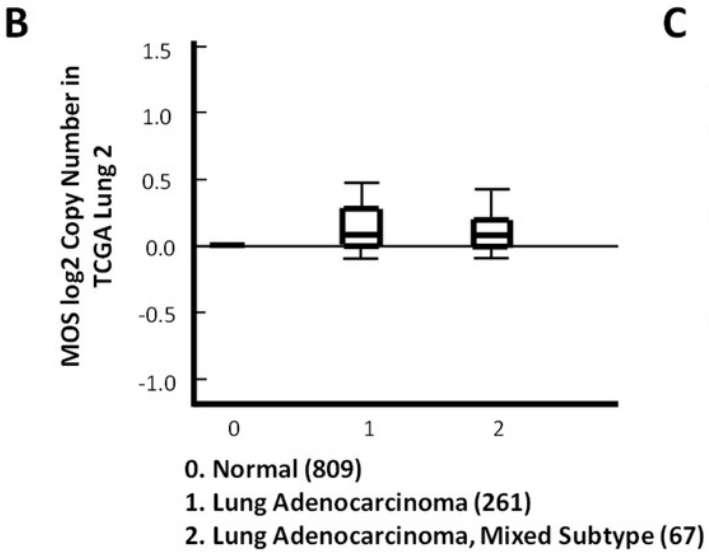
B
MOS log2 Copy Number in TCGA Lung 2
1.5
1.0
0.5
0.0
-0.5
-1.0
0
1
2
0. Normal (809)
1. Lung Adenocarcinoma (261)
2. Lung Adenocarcinoma, Mixed Subtype (67)

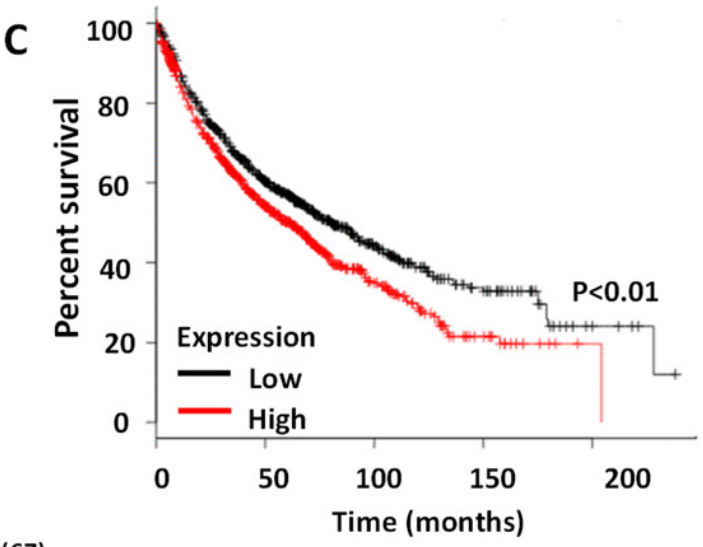
C
Percent survival
100
80
60
40
20
0
P<0.01
Expression
Low
High
0
50
100
150
200
Time (months)

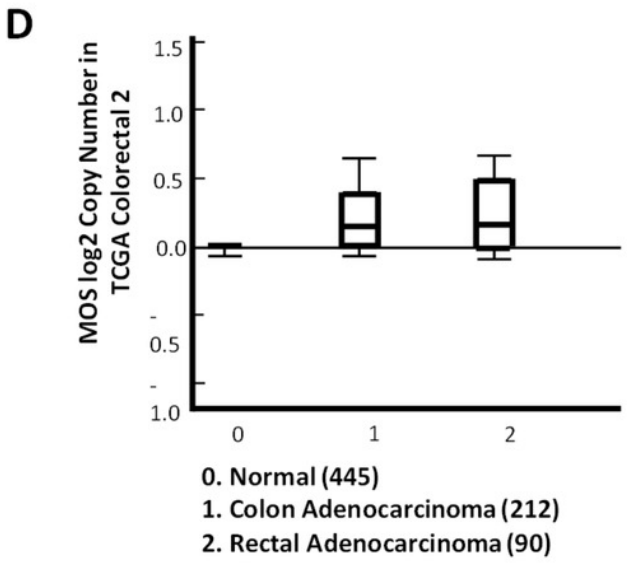
D
MOS log2 Copy Number in TCGA Colorectal 2
1.5
1.0
0.5
0.0
-0.5
-1.0
0
1
2
0. Normal (445)
1. Colon Adenocarcinoma (212)
2. Rectal Adenocarcinoma (90)

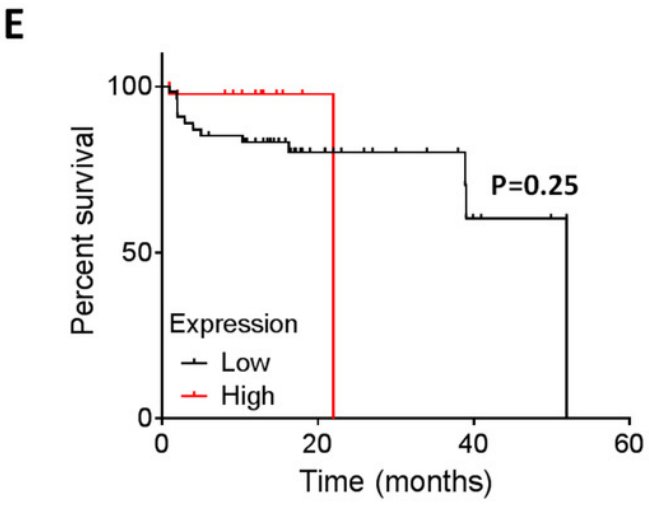
E
Percent survival
100
50
0
P=0.25
Expression
Low
High
0
20
40
60
Time (months)

Figure 3

Genetic deletion of c-mos gene has no effect on intestine and lung morphogenesis

(A) Real-time PCR quantification of c-mos mRNA levels in mouse lung and intestine tissues with wild-type (n=3) and with c-mos deficiency (n=3). Data were presented as means ± SEM. Statistical analyses were performed using Two-way ANOVA. (B) H&E staining of the lung from wild-type and c-mos-/- mice with regular architecture. (C) Representative H&E staining of intestine from wild-type and c-mos-/- mice intestine. Scale bars: 50μm. (D) Analysis of GeneAtlas MOE430, gcrma in the BioGPS database (http://biogps.org) revealed that c-mos expression is present in most mouse tissues but significantly higher in ovaries.

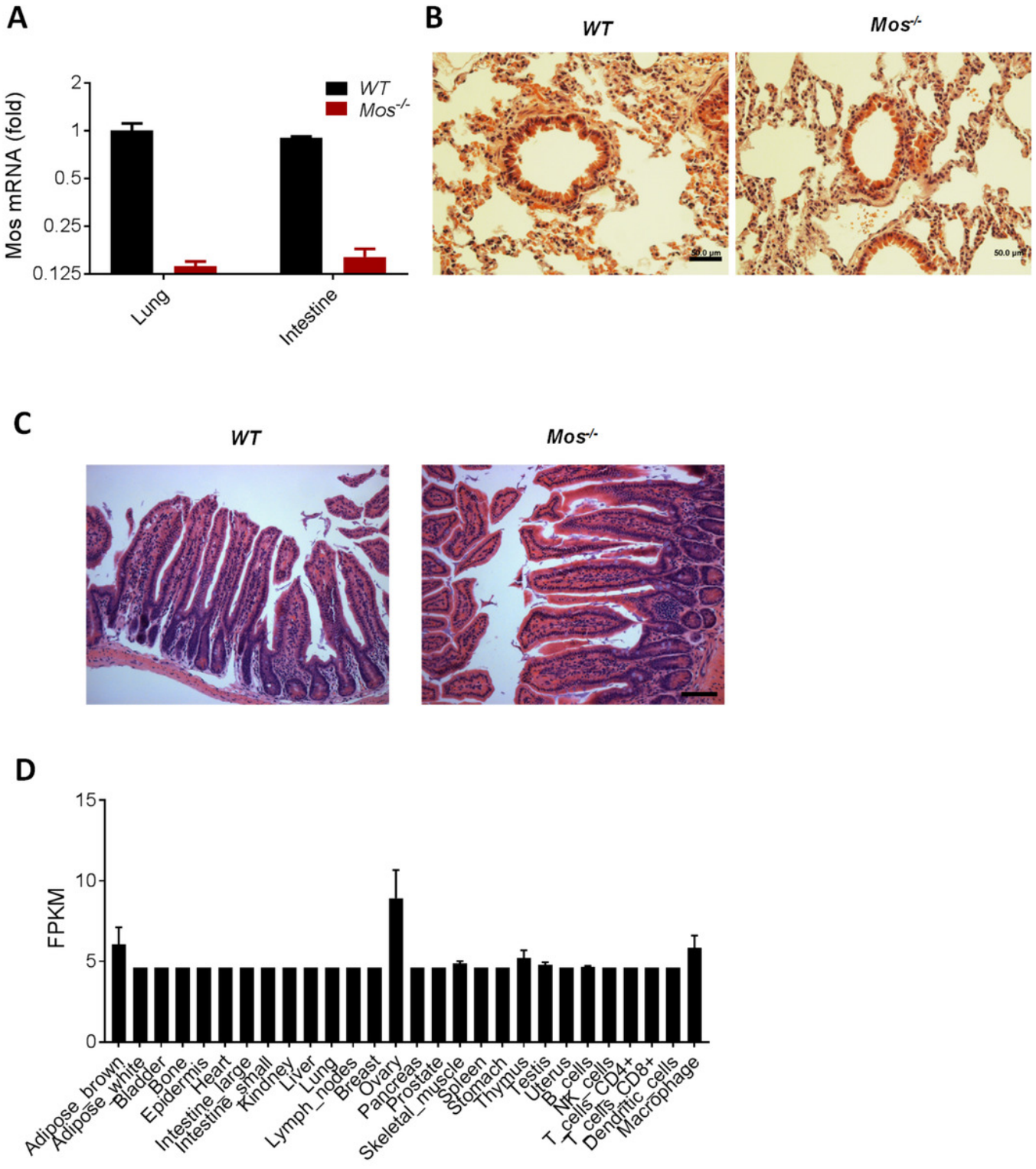
A
Mos mRNA (fold)
2
1
0.5
0.25
0.125
WT
Mos-/-
Lung
Intestine
B
WT
Mos-/-
50.0 μm
50.0 μm
C
WT
Mos-/-
D
FPKM
15
10
5
0
Adipose_brown
Adipose_white
Bladder
Bone
Epidermis
Heart
Intestine_large
Intestine_small
Kindney
Liver
Lung
Lymph_nodes
Breast
Ovary
Pancreas
Prostate
Skeletal_muscle
Spleen
Stomach
Thymus
Testis
Uterus
B_cells
NK_cells
T cells_CD4+
T cells_CD8+
Dendritic_cells
Macrophage

Figure 4

Genetic deletion of c-mos gene has on effect on tumor burden in both of KrasG12D lung cancer mice model and APCMin/+ intestine cancer mice model

(A-B) Tumor development in c-mos knockout and wild-type (WT) within KrasG12D mutation. Animals showed spontaneous lung tumor development at 5 months' age. A. Total number of lung surface tumor. (B) Number of large tumor based on tumor size (diameter >2 mm). (C) Histological confirmation of tumor development. Scale bars: 100µm. Data are presented as means ± SEM. N=9-11, Student's t-test. D-E. Tumor development in c-mos knockout and wild-type (WT) within APCmin/+ animals. Animals showed spontaneous intestine tumor development at 5 months' age. (D) Total number of small intestine tumors. E. Number of the intestine tumor based on polys size. (F) Total number of colon tumor. (G) Number of colon tumor based on polys size. Data are presented as means ± SEM. N=5, Two-way ANOVA.

PeerJ Preprints | https://doi.org/10.7287/peerj.preprints.3426v1 | CC BY 4.0 Open Access | rec: 22 Nov 2017, publ: 22 Nov 2017